Direct Shear Probe of Vortex Lattice Melting in $Bi_2Sr_2CaCu_2O_8$ Single Crystals

H. Pastoriza and P. H. Kes
Kamerlingh Onnes Laboratory, Rijksuniversiteit Leiden, P.O. Box 9506, 2300 RA, Leiden, The Netherlands
(Received 5 July 1995)

We report results of transport measurements on single crystals of the superconductor $Bi_2Sr_2CaCu_2O_8$ where weak pinning channels in a strong pinning environment were artificially introduced. The experimental data show that in this material the shear viscosity of the vortex liquid phase suddenly increases upon decreasing the temperature supporting the melting scenario. We also found that below the phase transition the data are in good agreement with plastic flow of a vortex solid through the channels.

PACS numbers: 74.60.Ge

Several vortex phases have been predicted to exist in layered high temperature superconductors [1,2]. The high critical temperature and the extreme anisotropy of these materials greatly enhance the role of thermal fluctuations in the phenomenological behavior of the vortex system. These fluctuations can lead to a loss of coherence between the superconducting layers resulting in two-dimensional vortex lattices in each layer, as well as induce melting of the vortex lattice giving a vortex liquid as a result. Recent susceptibility and dc-magnetization experiments showed the existence of a first order phase transition at low applied magnetic fields associated with the loss of coherence between planes [3,4]. On the other hand, neutron diffraction measurements revealed a sudden change in the correlation of the vortex ensemble [5] suggesting a melting transition at the irreversibility line in a similar temperature and field range.

Complementary to the change in long range correlations one can study the capability to sustain a shear stress. A sudden loss of this physical property will mark the transition from a vortex solid to a vortex liquid phase. In this work we use, in order to test the melting hypothesis, a dynamic approach to directly probe the shear strength of a vortex structure. The experimental data show that in $Bi_2Sr_2CaCu_2O_8$ the shear viscosity in the high temperature phase suddenly increases upon decreasing temperature, supporting the melting scenario. In addition, we observe that in the low temperature phase the data are in good agreement with plastic flow of the vortex lattice through the channels.

To probe the shear strength of the vortex structure transport measurements were carried out on samples in which weak-pinning channels were immersed in a strong-pinning environment. In this configuration it is possible to examine the restoring shear force of the vortices situated in the weak-pinning regions just by a resistance measurement with the applied current perpendicular to these channels. Flow of vortices in the channels occurs as soon as the critical stress of the vortex lattice at the channel edges is exceeded by the Lorentz force [6]. Within a continuum approximation the current density j_S which initiates the flow of vortices in these channels can be expressed as

$$j_S = 2Ac_{66}/WB, \tag{1}$$

where W is the width of the channel, A is a constant that takes into account anharmonicities in the lattice potential [7], and c_{66} is the shear modulus of the lattice given by

$$c_{66} = \frac{\Phi_0 B}{16\pi\mu_0\lambda_{ab}^2(t)}, \tag{2}$$

with B denoting the magnetic field, Φ_0 the flux quantum, and λ_{ab} the in-plane penetration depth.

The samples used in this work were prepared from $Bi_2Sr_2CaCu_2O_8$ single crystals grown by the traveling solvent floating zone technique [8]. These crystals have very good superconducting properties [5,9] and besides the bulk pinning is negligible above 40 K for the field range studied here [10]. The fabrication of the desired pinning pattern was done by irradiating the samples with high energy ions while covering the channel locations with a mask. It has been shown that this type of irradiation produces uniform cylindrical tracks of amorphous material in these compounds [11] which increments the pinning of vortices by about 1 order of magnitude. In our case we irradiated the crystals either with 5.9 GeV ^{208}Pb at GANIL (Caen, France) or 2.7 GeV ^{238}U at GIS (Darmstadt, Germany). In both cases the irradiation dose was 5×10^{10} ions/cm^2, equivalent to a matching field of 1 T, well above the fields used in this work.

A crucial part of the experiment is the design and fabrication of a mask suitable to stop the high energy ions in a grid of lines and let them pass in between. We constructed the masks by depositing an $\approx$2.5 μm layer of Au on a 12.5 μm Kapton foil. This bilayer was tightly rolled around a glass capillary tube and covered with epoxy. Subsequently, slices were cut from the cylinder and polished down to 200 μm [12]. In Fig. 1(a) we sketch the irradiation configuration. In order to check the effectiveness of the masks in stopping the high energy ions we performed selective etching of the columnar defects, either in the crystals with a solution of Na_2-EDTA [13] or with HF in the mica used as a holder

0031-9007/95/75(19)/3525(4)$06.00

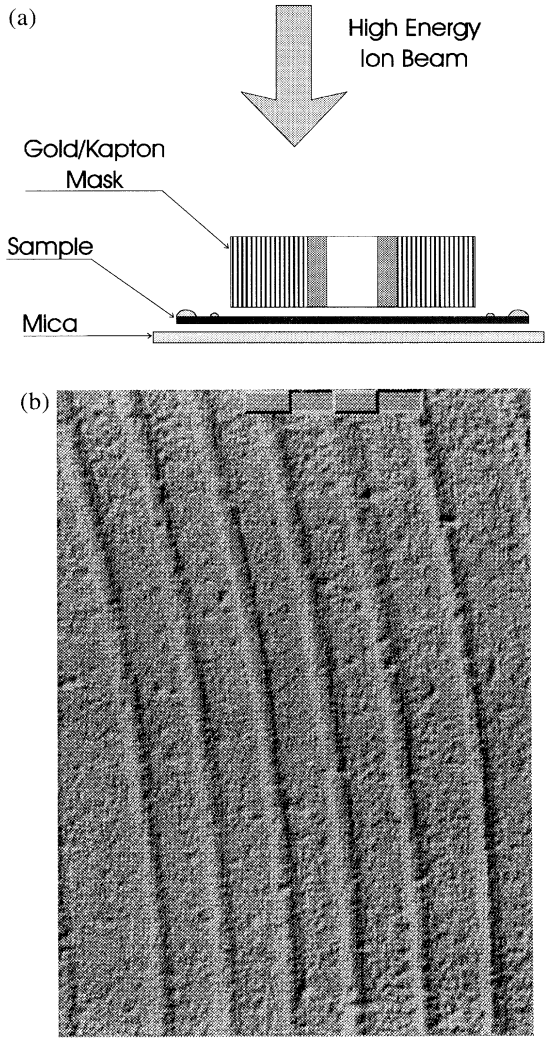

FIG. 1. (a) Sketch of the irradiation configuration. (b) Optical microphotograph of a mask-irradiated mica after etching with HF. The marks corresponds to 10 μm.

during the irradiation [see Fig. 1(a)]. In Fig. 1(b) we show an optical microphotograph of one of the etched mica substrates. This also allowed us to measure the final number and average width of the weak pinning channels in the samples.

The dc transport measurements were performed in a close-cycle refrigerator supplied with a Helmholtz solenoid capable of sustaining magnetic fields up to 1.4×10^5 A/m (1.5 kOe). All data were taken in the standard four probe configuration. Care was taken to contact the side of the crystals with the outer pads in order to obtain a uniform current distribution inside the sample. Sample sizes were $0.02 \times 0.22 \times 4.10$ mm^3 and the distance between the voltage contacts was 3.5 mm. All measurements were taken during cooling of the sample in the presence of the magnetic field.

Shown in the inset of Fig. 2 are the zero field transitions of one of the samples before and after the irradiation

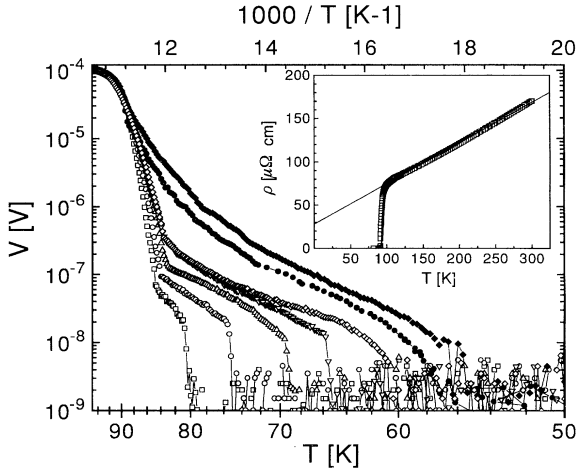

FIG. 2. Arrhenius plot of the voltage vs temperature for selected magnetic fields. The measuring current density was 1×10^6 A/m^2. □: 10 mT, ○: 20 mT, △: 30 mT, ▽: 40 mT, ◇: 50 mT. Filled symbols: before irradiation. Open symbols: after irradiation. Inset: Zero field transition in a extended range of temperatures. Symbols: before irradiation. Solid line: after irradiation. Dotted line: linear fit to the normal state resistance.

with 2.7 GeV ^{238}U ions. As is clearly seen there were no changes in the sample resistance in the whole range of temperatures, or in T_C (90.5 K) either in the transition width or the normal state resistivity.

In Fig. 2 we show an Arrhenius plot of the voltage as a function of temperature for different applied magnetic fields taken with a current density of 1×10^6 A/m^2. For comparison we also plot the measurements at two selected fields for the same sample before the irradiation. The qualitative behavior, and main features of this work, can be extracted from this figure. Prior to irradiation the resistive transitions are widened by the magnetic field as is well known and previously reported [14]. In contrast, it is clearly seen that after the irradiation the transition to the zero resistance state is given by two contributions. At high temperatures there is a sharp decrease of the resistivity associated with the trapping of vortices by the columnar defects. Below a well-defined field-dependent temperature T_{bg}, the behavior changes to a temperature dependence with a much lower activation energy, similar to that in the unirradiated sample. Considering that in this range of temperatures the irradiated and nonirradiated regions essentially contribute as two resistors in series we can estimate the ratio $V_i/V_c \simeq n_{\rm ch}W/l$, where V_i is the voltage in the irradiated sample, and V_c is the voltage in the nonirradiated crystal, $n_{\rm ch}$ and W are the number and average width of the channels, and l is the distance between contacts. Using the measured values $n_{\rm ch} = 60 \pm 5$, $W = 3 \pm 0.2$ μm, and $l = 3.49$ mm, we get 5.1×10^{-2} in agreement with the measured ratio. It is clear then that in this temperature range the voltage is produced by the movement of the vortex liquid inside the weak-pinning channels.

Further lowering of the temperature shows for all fields below 450 Oe a sudden drop of the resistance to zero, in obvious contrast with the response of the nonirradiated sample. For higher fields no jump could be observed above the minimum voltage resolution of our setup. This jump in the voltage is clear evidence that the vortex motion inside the channels is abruptly blocked. Following the description of Nelson and Halperin [15], the sudden decay sets in when the shear viscosity of the liquid starts to grow upon approaching the liquid-solid phase transition. In a two-dimensional system the shear viscosity $\eta(T) \propto \xi_+^2(T)$, where the correlation length of the liquid $\xi_+(T)$ is given by

$$\xi_+ \simeq \xi_{+0} \exp\left[b \left(\frac{T_m}{T - T_m} \right)^{\nu} \right]. \quad (3)$$

Here b is a nonuniversal constant of order unity, ν is the critical exponent, $\nu = 0.369\,63\ldots$, T_m is the melting temperature, and ξ_{+0} represents the smallest characteristic length scale in the liquid and therefore $\xi_{+0} \approx a_0$, with a_0 the vortex lattice parameter. In our case the system under investigation consists of a vortex ensemble constrained inside a narrow channel. Here the characteristic feature of the melting transition is going to be observed when the correlation length of the liquid reaches the width of the channel, i.e., $\xi_+(\tilde{T}_m) = W$, where $\tilde{T}_m$ is the temperature at which the voltage jump is observed. The real melting temperature may thus be somewhat lower than the $\tilde{T}_m(H)$ values we obtain in our experiment [16].

In the H-T phase diagram shown in Fig. 3 we have plotted the various transition temperatures obtained in this experiment. The open circles display the temperatures where trapping of vortices in the columnar defects occurs. These points basically mark the change in the dynamics of vortices in the presence of columnar defects related to a transition from the Bose-glass state to a flux-creep dominated behavior above the depinning temperature [17]. The solid squares denote the temperatures where the melting of the vortex system takes place and the open squares where the resistance of the sample vanishes continuously below the resolution level. For comparison we have added the results obtained by neutron diffraction [5], and muon-spin rotation (μSR) experiments [9] on similar crystals. The neutron diffraction data denote the fields or temperatures at which the integrated intensity of the six diffraction lines quickly disappears. The μSR data are determined from a sudden sign change of the asymmetry of the field distribution. Also shown are the previously reported data on crystals of other origin. The data by Pastoriza *et al.* [3] are defined by the loss of phase coherence along the c direction while those of Zeldov *et al.* [4] represent the place at which a step in the flux density is observed.

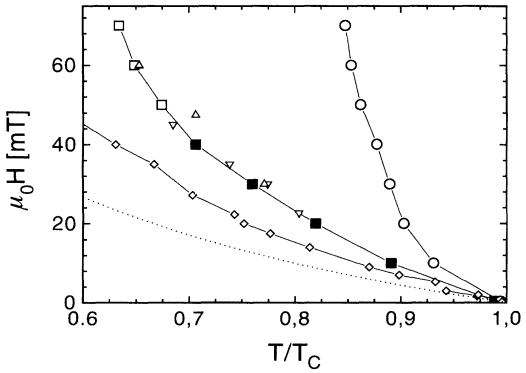

FIG. 3. Phase diagram for the irradiated $Bi_2Sr_2CaCu_2O_8$ single crystal composed from the data shown in Fig. 2. ○: depinning field, B_{bg}, in the irradiated regions, ■: melting field, △: melting field as determined by neutron diffraction [5], ▽: melting field from muon-spin rotation [18], ◇: phase transition after [3]. Dotted line: after [4].

The line shift between crystals of different origin is due to variations in oxygen content which arises because of nonidentical growth and/or anneal conditions. It is well known that different oxygen concentrations change the transition temperature, the anisotropy, and the penetration depth. Very recent experiments with Hall probe arrays [19] on single crystals with different oxygen contents show indeed that a relative change of oxygen concentration of 0.3% causes a line shift by a factor of 2. Our data were obtained on crystals that have been annealed for 6 h in air at 500 °C.

Considering all collected data the conclusion emerges that all experimental techniques determine the same transition. Since these techniques provide both evidence for a phase transition [3,4] and a decoupling of the superconducting layers [3], it seems that in Bi-2212 the melting and decoupling lines coincide. This conclusion justifies the description of the voltage decay given above, since the vortex ensemble above the transition line will behave as a two-dimensional liquid.

Finally we show in Fig. 4 I-V characteristics at 80 K for different applied magnetic fields on a logarithmic scale. We find three different regimes depending on the magnetic field. At high magnetic fields the response is linear in the

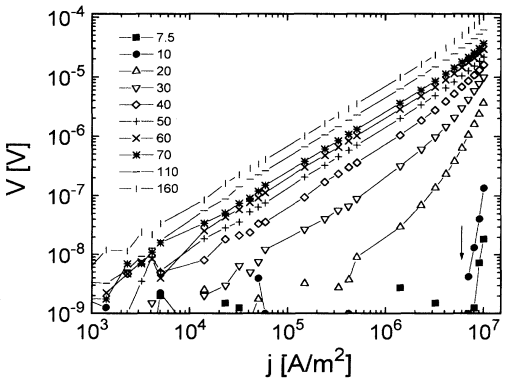

FIG. 4. I-V characteristics for the irradiated sample at different magnetic fields. The numbers indicate the magnetic field in mT. The arrow marks the estimated shear current j_S.

whole current range (line symbols). For fields lower than B_{bg} (open symbols) the response becomes nonlinear but with a finite resistivity when the applied current density approaches zero. Further lowering the field below the melting field (solid symbols) an almost field independent finite critical current appears, denoted by the arrow in the figure, below which no dissipation is detected. We can identify this critical current with the shear current density j_S needed to overcome the interaction of the vortex lattice with the channel boundaries. Using Eqs. (1) and (2) and $\lambda_{ab} = \lambda_{ab}(0)/\sqrt{1-t}$, $\lambda_{ab}(0) = 140$ nm, and $j_S = 6 \times 10^6$ A m^{-2}, we obtain a value for $A = 0.05$, in excellent agreement with previous estimates based on the peak effect observed in 2D collective-pinning experiments [6,20].

In conclusion, we have presented transport measurements on $Bi_2Sr_2CaCu_2O_8$ single crystals where vortices are forced to flow in constrained channels directly probing the shear strength of the vortex system. These results show that coincident with the irreversibility line at low fields, in this compound, there is a melting of the vortex structure. This was observed by the sudden increase of the shear viscosity in the liquid phase. We have also found a good agreement with the continuum approximation for the shear strength of the vortex lattice.

We would like to acknowledge the valuable contribution of C. W. Hagen at the early stages of this project and M. Konczykowsky for his valuable advice and the assistance in the irradiation at GANIL and J. Weissner and G. Wirth for the irradiation at GIS. This work is part of the research program of the "Stichting voor Fundamenteel Onderzoek der Materie," which is financially supported by NWO and a EU grant under Contract No. CL1-CT930069.

[1] L. I. Glazman and A. E. Koshelev, Phys. Rev. B **43**, 2835 (1991).

[2] G. Blatter, M. V. Feigel'man, V. B. Geshkenbein, A. I. Larkin, and V. M. Vinokur, Rev. Mod. Phys. **66**, 1125 (1994).

[3] H. Pastoriza, M. F. Goffman, A. Arribére, and F. de la Cruz, Phys. Rev. Lett. **72**, 2951 (1994).

[4] E. Zeldov, E. Majer, M. Konczykowski, V. B. Geshkenbein, V. M. Vinokur, and H. Shtrikman, Nature (London) **375**, 373 (1995).

[5] R. Cubitt, E. M. Forgan, G. Yang, S. L. Lee, D. McK. Paul, H. A. Mook, M. Yethhiraj, P. H. Kes, T. W. Li, A. A. Menovsky, Z. Tarnawski, and K. Mortensen, Nature (London) **365**, 407 (1993).

[6] A. Pruymboom, P. H. Kes, E. van der Drift, and S. Radelaar, Phys. Rev. Lett. **60**, 1430 (1988).

[7] R. Schmucker, Philos. Mag. **35**, 431 (1977).

[8] T. W. Li, P. H. Kes, N. T. Hien, J. J. M. Franse, and A. A. Menovsky, J. Cryst. Growth **135**, 481 (1994).

[9] S. Lee, P. Zimmermann, H. Keller, M. Warden, I. M. Savić, R. Schuwecker, D. Zech, R. Cubitt, E. M. Forgan, P. H. Kes, T. W. Li, A. A. Menovsky, and Z. Tarnawski, Phys. Rev. Lett. **71**, 3862 (1993).

[10] M. V. Indenbom, G. D'Anna, M.-O. André, W. Benoit, H. Kronmüller, T. W. Li, and P. H. Kes, in *Proceedings of the 7th International Conference on Critical Currents in Superconductors, Alpbach, 1994,* edited by H. W. Weber (World Scientific, Singapore, 1994), p. 327.

[11] L. Civale, A. D. Marwick, T. K. Worthington, M. A. Kirk, J. R. Krusin-Elbaum, Y. Sun, J. R. Clem, and F. Holzberg, Phys. Rev. Lett. **67**, 648 (1991); W. Gerhäuser, G. Ries, H. W. Neumüller, W. Schmidt, O. Eibl, G. Saemann-Ischenko, and S. Klamnzer, Phys. Rev. Lett. **68**, 879 (1992).

[12] The stopping range in gold for 5.9 GeV Pb ions is estimated to be 75.5 μm, while they go through the Kapton leaving the mask with an energy of about 4.5 GeV. In the case of 2.7 GeV ^{238}U ions these numbers are 35 μm and 0.6 GeV, respectively.

[13] H. Dai, S. Yoon, J. Liu, R. C. Budhani, and C. M. Lieber, Science **265**, 1552 (1994).

[14] T. T. M. Palstra, B. Batlogg, R. B. van Dover, L. F. Schneemeyer, and J. V. Waszczak, Phys. Rev. B **41**, 6621 (1990).

[15] D. R. Nelson and B. I. Halperin, Phys. Rev. B **19**, 2457 (1979).

[16] From similar experiments carried out in Nb_3Ge amorphous films we get an estimation of $b = 0.5$ and $\xi_{+0} = 0.6a_0$ which implies that this shift is 1.6% at 10 mT and 0.8% at 40 mT. Martijn Theunissen (private communication).

[17] C. J. van der Beek, M. Konczykowski, V. M. Vinokur, G. W. Crabtree, T. W. Li, and P. H. Kes, Phys. Rev. B **51**, 15 492 (1995).

[18] S. L. Lee, M. Warden, H. Keller, J. W. Schneider, D. Zech, P. Zimmermann, R. Cubitt, E. M. Forgan, M. T. Wylie, P. H. Kes, T. W. Li, A. A. Menovsky, and Z. Tarnawski, Phys. Rev. Lett. **75**, 922 (1995).

[19] B. Khaykovich, E. Zeldov, D. Mayer, T. W. Li, P. H. Kes, and M. Konczykowski (unpublished).

[20] R. Wördenweber, P. H. Kes, and C. C. Tsuei, Phys. Rev. B **33**, 3172 (1986).

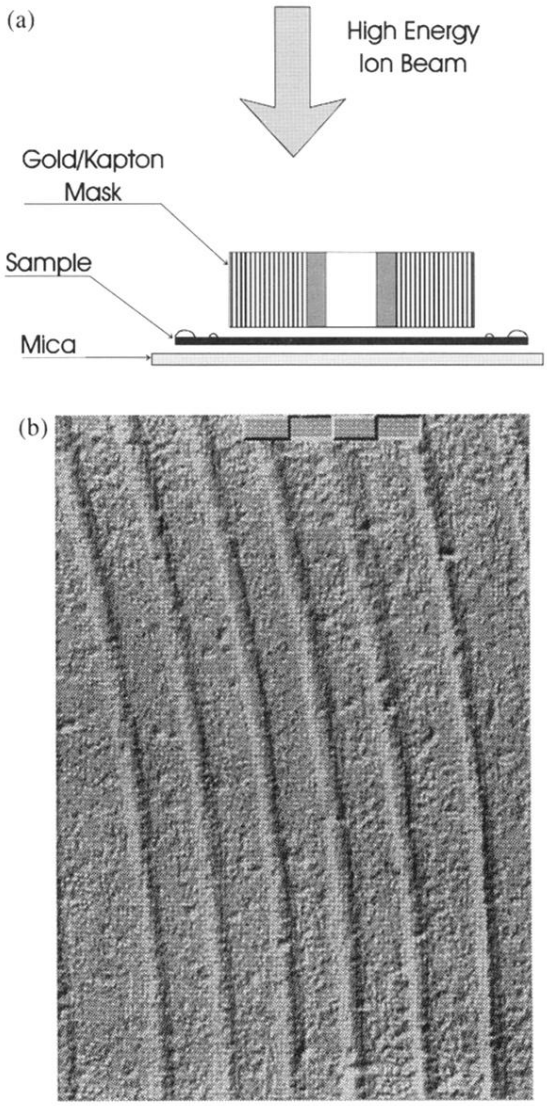

FIG. 1. (a) Sketch of the irradiation configuration. (b) Optical microphotograph of a mask-irradiated mica after etching with HF. The marks corresponds to 10 μm.